Probing Determinants of the Metal Ion Selectivity in Carbonic Anhydrase Using Mutagenesis†

Keith A. McCall‡,§ and Carol A. Fierke*,||

Department of Biochemistry, Duke University Medical Center, Box 3711, Durham, North Carolina 27710, and Department of Chemistry, University of Michigan, 930 North University Avenue, Ann Arbor, Michigan 48109-1055

Received January 14, 2004; Revised Manuscript Received February 2, 2004

ABSTRACT: Few studies measuring thermodynamic metal ion selectivity of metalloproteins have been performed, and the major determinants of metal ion selectivity in proteins are not yet well understood. Several features of metal ion binding sites and metal coordination have been hypothesized to alter the transition metal selectivity of chelators, including (1) the polarizability of the coordinating atom, (2) the relative sizes of the binding site and the metal ion, and (3) the metal ion binding site geometry. To test these hypotheses, we have measured the metal ion affinity and selectivity of a prototypical zinc enzyme, human carbonic anhydrase II (CAII), and a number of active site variants where one of the coordinating ligands is substituted by another side chain capable of coordinating metal. CAII and almost all of the variants follow the inherent metal ion affinity trend suggested by the Irving−Williams series, demonstrating that this trend operates within proteins as well as within small molecule chelators and may be a dominant factor in metal ion selectivity in biology. Neither the polarizability of the liganding side chains nor the size of the metal ion binding site correlates strongly with metal ion specificity; instead, changes in metal ion specificity in the variants correlate with the preferred coordination number and geometry of the metal ion. This correlation suggests that a primary feature driving deviations from the inherent ligand affinity trend is the positioning of active site groups such that a given metal ion can adopt a preferred coordination number/geometry.

Many proteins contain tightly bound metal ions, including a number of transition metals (e.g., Mn, Fe, Co, Cu, Zn, and Mo) (*1*). In many cases, the identity of the metal ion is crucial for the biological function of the protein, and therefore, it is essential that the correct metal ion be incorporated in vivo. Incorporation of the correct metal is dependent on the concentration of metal ions in vivo and either kinetic or thermodynamic metal ion selectivity. Even where metallochaperones deliver the metal ion, selectivity is still required; the chaperone must acquire and deliver the correct metal ion, and the metalloenzyme must accept and retain the correct metal ion while not accepting or retaining inappropriate metal ions. So far, few studies measuring thermodynamic metal ion selectivity have been performed, and the major determinants of metal ion selectivity in proteins are not yet well understood.

In small molecule chelators a general trend in metal ion affinity ($Mn^{2+} < Co^{2+} < Ni^{2+} < Cu^{2+} > Zn^{2+}$), termed the Irving−Williams series (*2*), is frequently observed and correlates with the second ionization enthalpy (*3*) of the divalent ions of the metal. Several features of metal ion binding sites have been hypothesized to alter the transition metal selectivity of chelators, including (1) the polarizability of the coordinating atom [hard−soft/acid−base theory (*4*, *5*)], (2) the relative sizes of the binding site and the metal ion, and (3) the metal ion binding site geometry or the site's ability to provide the preferred coordination number (*6*, *7*).

To test the importance of these hypotheses for metal ion selectivity in proteins, we measured the metal ion affinity and selectivity of a prototypical zinc enzyme, human carbonic anhydrase II (CAII),[1] and a number of active site variants of this enzyme. The His_3 zinc polyhedron of CAII (Figure 1) is capable of binding a wide range of metal ions. In each case, the metal ion coordination in metal-substituted CAII (*8*, *9*) is the characteristic coordination geometry typically found for these metals in protein crystal structures; i.e., manganese and nickel are both octahedral, while cobalt and zinc are both tetrahedral. Cu^{2+} bound to proteins is typically either in a distorted 4-coordinate geometry intermediate between tetrahedral and square planar (*10*, *11*) or in a face-centered trigonal pyramidal geometry (*12*). Additionally, in both cases a water molecule is within 2.8−2.9 Å of the metal ion, in position to form a trigonal bipyramidal geometry (*13*, *14*). As expected, Cu^{2+} bound to CAII adopts the typical

† This work has been supported by NIH Grant GM 40602. K.A.M. was supported in part by an ASSERT award from the Office of Naval Research (N00014-95-1-0951).

* To whom correspondence should be addressed. Telephone: 734-936-2678. Fax: 734-647-4865. E-mail: fierke@umich.edu.

‡ Duke University Medical Center.

§ Current address: Division of Hematology, University of Utah, 30 North 1900 East, Salt Lake City, UT 84132-2408.

|| University of Michigan.

[1] Abbreviations: CAII, human carbonic anhydrase II; Azm, acetazolamide or *N*-(5-sulfamoyl-1,3,4-thiadiazol-2-yl)acetamide; DPA, iminobis(methylene-2-pyridine) or dipicolinic acid; MOPS, 3-(*N*-morpholino)propanesulfonic acid; PAR, 4-(2-pyridylazo)resorcinol; PNPA, *p*-nitrophenyl acetate; Tris, tris(hydroxymethyl)aminomethane; WT, wild type.

10.1021/bi0498914 CCC: $27.50
Published on Web 03/06/2004

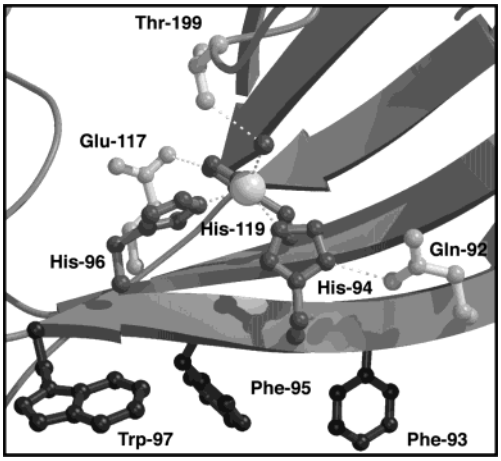

FIGURE 1: Metal binding site of wild-type CAII. The geometry of Zn^{2+} bound to wild-type CAII is tetrahedral. This figure was generated in Molscript (*43*) from the crystal structure of wild-type CAII (*9*) and then rendered with Raster3D (*44*).

distorted 4-coordinate geometry, with a distant oxygen from a second water molecule in a position to form a trigonal bipyramidal geometry (*8*).

The metal ion selectivity of wild-type CAII follows the Irving−Williams series, although the affinity of Zn^{2+} is near that of Cu^{2+} and is increased significantly compared to the rest of the transition metals (*15*, *16*). To investigate the determinants of metal ion selectivity, we measured the metal ion affinity and specificity of CAII variants where one of the coordinating His ligands (either H94, which coordinates through the Nϵ2 atom, or H119, which coordinates through the Nδ1 atom) was substituted by another side chain capable of coordinating Zn^{2+}, including Asp, Glu, Gln, Asn, and Cys. In almost every case, the metal ion selectivity of the variants also follows the Irving−Williams series, demonstrating that the second ionization energy of the metal ion (3) is a dominant factor in thermodynamic metal ion selectivity in proteins, although other influences can alter this trend. These data also indicate that the polarizability of the coordinating atom (S vs O) is not a major factor in metal ion selectivity in CAII. Furthermore, site size is important for metal discrimination only when the ionic radii of the metals are significantly different, for example, in discriminating between Cd^{2+} (1.09 Å) and Zn^{2+} (0.88 Å). Most importantly, these data demonstrate that changes in metal ion specificity of the variants correlate with the preferred coordination number and geometry of the metal ion, as observed in protein crystal structures. Therefore, we conclude that the primary features driving deviations from the inherent ligand affinity trend, i.e., the Irving−Williams series, are those that alter the energy required for a bound metal ion to adopt a preferred coordination number and geometry.

MATERIALS AND METHODS

Preparation of Plasticware and Solutions. All plasticware, including dialysis clips, was initially acid-washed and then soaked with a 50 mM cadmium solution to replace readily exchangeable metal ions in the plasticware. Thereafter, and between each use, the plasticware was soaked in a 4 mM (ethylenedinitrilo)tetraacetic acid solution overnight and rinsed thoroughly with deionized water (18 MΩ). No metal was observed to leach out of the plasticware after this treatment. All solutions were prepared in treated plasticware using deionized water (18 MΩ) and metal-free pipet tips (Bio-Rad) to minimize metal ion contamination. All reagents, buffers, and solvents were of the highest purity available. The Mn^{2+}, Co^{2+}, Ni^{2+}, Cu^{2+}, and Cd^{2+} metal ion solutions used in the standard curves and metal ion buffer solutions were atomic absorption standards ($\sim$1000 μg/mL in 1 wt % HNO_3; Aldrich). The Zn^{2+} metal ion solution was a $ZnSO_4$ volumetric standard (0.0499 M solution in water; Aldrich).

Preparation of Metal Ion Buffers. Metal ion buffers were prepared with bicine (Aldrich) or citric acid (Mallinckrodt). Additionally, trace amounts (4−6 μM) of dipicolinic acid (DPA) were included to ensure rapid equilibration of the metal ion with CAII (*17*). The pH of the solution was adjusted to 7.0 with semiconductor grade NaOH (pellets, 99.99%; Aldrich), and 3-(*N*-morpholino)propanesulfonic acid (MOPS) was added to maintain the total combined buffer concentration at 15 mM. The buffer combinations and concentrations were chosen such that >90% of the total metal ion is chelated by the buffers. The concentration of free metal ion at a particular pH and buffer concentration was calculated from the known stability constants of the buffers (*18*).

Colorimetric and Fluorescent Metal Ion Assays. The colorimetric and fluorescent assays to determine metal ion concentration were performed as previously described (*15*). First, the metal standard solution or the protein solution is diluted into a denaturing solution (final concentration = 4 M guanidine hydrochloride, 7.5 mM MOPS, pH 7.0) and incubated for 2−3 min at room temperature to allow the protein to unfold (*19*). Then a freshly prepared solution of 4-(2-pyridylazo)resorcinol (PAR, final concentration = 100 μM) is mixed with the sample, and the absorbance is immediately determined at 500 nm (Ni^{2+} and Zn^{2+}) or 514 nm (Co^{2+} and Cu^{2+}). The metal concentration is determined by comparison to a standard curve (0−10 μM). To measure the concentration of Mn^{2+} and Cd^{2+}, 20 μM Fura-2 (Molecular Probes) is used in place of PAR. The fluorescence is determined at an emission wavelength of 510 nm (Mn^{2+}) or 465 nm (Cd^{2+}) and at excitation wavelengths of 340 and 380 nm (Mn^{2+}) or 340 and 373 nm (Cd^{2+}). The metal ion concentration in the samples was determined by comparison to a standard curve (0−10 μM). Either apoenzyme was included in the standard curve (equimolar to the sample protein concentration) or several sample protein concentrations were examined.

Enzyme Preparation. The human CAII variants were prepared and purified as previously described (*20*, *21*). Fresh apoenzyme ($\sim 5 \times 10^{-7}$ mol per preparation) was prepared by Amicon diaflow filtration against DPA, as previously described (*22*). The bound zinc ion concentration was determined by the PAR assay (see above), and the apoenzyme preparation was used only if ≥90% of the bound metal ion was removed.

Determination of Binding Affinity. Dissociation constants (K_Ds) for metal ions were determined as previously described (*15*) by dialyzing apo-CAII (0.5 mL of 60−80 μM protein) against a larger volume (500 mL) of various concentrations of free metal ions, maintained by metal−chelator buffers which included ≥4 μM DPA at pH 7.0, for 16−22 h at 30 °C. Concentrations of free metal ions ($[M]_{free}$) were calculated as described above. Citrate was used as the primary chelator for Mn^{2+}, Co^{2+}, or Ni^{2+}, bicine was used as the primary

chelator for Cu^{2+}, and tris(hydroxymethyl)aminomethane (Tris) with high concentrations (0.2−10 mM) of DPA was used to buffer Zn^{2+} or Cd^{2+}. The total metal ion concentration was maintained at >40-fold above the total protein concentration to prevent any alteration in free metal ion concentration by sequestration in the protein. The protein-bound metal was dependent on the free metal ion concentration and independent of the total metal ion and total buffer concentration. The dialysis bags (Spectra/Por metal-free CE Membranes, MWCO 15000) were rinsed thoroughly with deionized water (18 MΩ) before use. Multiple proteins were simultaneously dialyzed against the same solution. After equilibration, unbound metal ions were removed from the sample solutions by gel filtration over a PD-10 column (Sephadex G-25M, 5 cm × 15 cm; Pharmacia). Varying the length of equilibration from 16 to 22 h had no effect on the observed metal ion affinity. The enzyme concentration ($[E]_{tot}$) was determined from absorbance (*23*), and the bound metal concentration ([E·M]) was measured by either the PAR colorimetric assay (Co^{2+}, Ni^{2+}, Cu^{2+}, and Zn^{2+}) or a fluorescent Fura-2 assay (Mn^{2+} and Cd^{2+}), as detailed above. The dissociation constant and asymptotic standard error were calculated using the program KaleidaGraph (Synergy Software) from a fit of eq 1 to the data, where the end point, *C*, varied from 0.7 to 1.3.

$$[E\cdot M]/[E]_{tot} = C/(1 + K_D/[M]_{free}) \quad (1)$$

In each case, the equilibration and metal ion binding assay was repeated two to four times, both to cover a free metal ion concentration range spanning both the high and low plateaus of the binding curve and to improve the accuracy of the dissociation constant (K_D) determination.

RESULTS AND DISCUSSION

The apparent stability constants of various metal ions bound to proteins have been determined for several metalloenzymes, including carboxypeptidase A (*24*), human carbonic anhydrase I (*16*), pro-carboxypeptidase A (*25*), and alcohol dehydrogenase (*26*). However, it is difficult to ascertain metal ion specificity rules from these data sets because the structure, composition, and binding site environments of the proteins are quite different from one another. For this reason, we measured the metal affinity of a set of proteins that differ by only one amino acid for a set of metal ions which neighbor each other on the periodic table (Mn^{2+}, Co^{2+}, Ni^{2+}, Cu^{2+}, Zn^{2+}, and Cd^{2+}), thereby systematically investigating the specificity and avidity of a number of closely related metal ion binding sites. These data then allow examination of the importance of several parameters (i.e., the Irving−Williams series, liganding atom polarizability, site size, site geometry) for determining metal ion specificity in CAII.

Metal Ion Affinity of the Variants. To examine the molecular determinants of metal ion specificity, we measured the metal ion affinity of both wild-type (WT) CAII and CAII variants using equilibrium dialysis followed by analysis of bound metal ions (Figure 2; Table 1). In the CAII variants, one of the three histidine ligands was substituted with Asp, Glu, Asn, Gln, or Cys at either position 94 or position 119 to form a novel metal ion polyhedron. The biologically important metal ions investigated in this work vary either in the number of valence electrons while maintaining similar ionic radius (Mn^{2+}, Co^{2+}, Ni^{2+}, Cu^{2+}, Zn^{2+}) or in the ionic radius while maintaining the same valence electron configuration (Zn^{2+} vs Cd^{2+}).

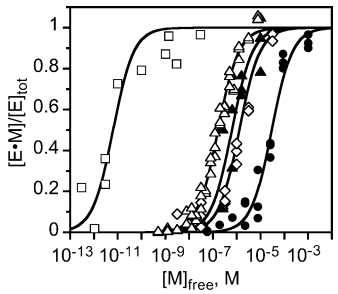

FIGURE 2: Metal ion affinity of H119N CAII. The metal ion dissociation constant was obtained by dialyzing 0.5 mL of 80 μM H119N CAII for 16−20 h at 30 °C against 500 mL of metal ion buffer used to maintain the free metal ion concentration. The affinity of the following metals was analyzed: Co^{2+} (●), Ni^{2+} (◇), Cu^{2+} (□), Zn^{2+} (△), and Cd^{2+} (▲). Enzyme-bound metal (E·M) was separated from free metal by chromatography on gel filtration columns and quantitated using either the PAR colorimetric or Fura-2 fluorometric assay, as described. The data shown here are representative of that from each of the variants. The background has been subtracted from each data set, and the end points have been normalized to 1. A binding isotherm was fit to the data (eq 1), and the values of K_D are listed in Table 1.

The determination of metal ion affinity for the variant enzymes was conducted at low ionic strength ($I \leq 0.1$) by dialysis against large volumes of metal ion buffers and at physiologically relevant pH (7.0) and temperature (30 °C). To reduce or remove artifacts from the data, all binding constants were determined directly for each metal ion rather than by competition. Furthermore, metal ion buffers were used to maintain the free metal ion concentration. Finally, to increase efficiency and improve the accuracy of determining the relative metal affinity of the variants, multiple proteins were simultaneously dialyzed against the same metal−buffer solutions. Therefore, even in the case of slight variations in pH, metal ion concentration, or temperature between experimental runs, the fractions of metal bound to the variant proteins (and hence the affinities) are directly comparable. The dialysis experiments were repeated until there were sufficient data so that the affinity order was clear and the error in the K_D was low (~±30% of the K_D) (Table 1). As an example of the quality of these data, the metal ion binding isotherms for the H119N CAII variant are shown in Figure 2. As in WT CAII (*15*), the weak affinity of the variants for Mn^{2+} allows the determination of only a lower limit of the K_D for Mn^{2+}. Similarly, the metal ion affinity of some of the variants decreased so significantly that we were only able to measure a lower limit for the metal affinity. The majority of the apo-CAII variants are stable enough that little (<20%) of the protein precipitates during the 16−22 h incubation at 30 °C. However, significant precipitation (up to 75%) of the H119Q variant was observed at high free copper concentrations (>1 μM), perhaps due to copper-mediated aggregation (*27*). Therefore, we were able to determine only a lower limit for the copper affinity in this case.

General Trends. Any change in the direct ligands from the wild-type His_3 metal polyhedron decreases metal ion affinity overall (e.g., metal ion binding to WT CAII is >16000-fold tighter than to H94E CAII, on average) but

Table 1: Affinity of a Series of Divalent Metal Ions for CAII Variants[a]

	pK_D[a]					
variant	Mn^{2+}	Co^{2+}	Ni^{2+}	Cu^{2+}	Zn^{2+}	Cd^{2+}
CAII	<3.4	6.8 ± 0.2	7.8 ± 0.2	13.0 ± 0.1	12.0 ± 0.1	8.64 ± 0.07
H94D	<3.0	6.36 ± 0.08	7.8 ± 0.1	11.28 ± 0.08	8.30 ± 0.07	8.46 ± 0.04
H94E	<3.0	<2.2	5.2 ± 0.2	11.4 ± 0.1	7.37 ± 0.07	5.9 ± 0.1
H94N	<3.0	2.0 ± 0.3	4.8 ± 0.2	11.00 ± 0.07	5.0 ± 0.2	<5.0
H94Q	<3.0	<2.4	5.6 ± 0.3	10.79 ± 0.06	6.15 ± 0.09	<4.2
H119D	ND[b]	3.9 ± 0.1	5.2 ± 0.1	10.1 ± 0.3	6.24 ± 0.03	5.8 ± 0.5
H119E	ND	<2.5	5.0 ± 0.2	8.6 ± 0.1	5.6 ± 0.1	<4.1
H119N	ND	4.53 ± 0.08	5.9 ± 0.1	11.3 ± 0.4	6.78 ± 0.05	6.2 ± 0.1
H119Q	ND	<2.5	<3.7	<6.0	6.00 ± 0.04	<3.9
H94C	ND	ND	ND	ND	6.6 ± 0.1	<4.3
H96C	ND	ND	ND	ND	5.48 ± 0.06	<3.1
H119C	ND	ND	ND	ND	6.8 ± 0.1	3.8 ± 0.3

[a] pK_D = −log K_D. Measurements were done at pH 7.0, 30 °C. [b] ND = not determined.

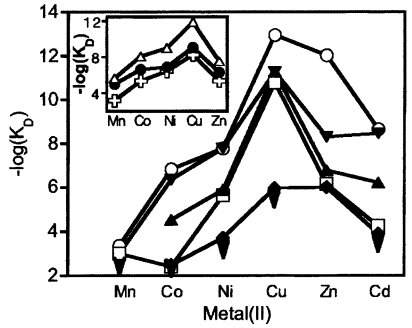

FIGURE 3: Metal ion affinity profiles of small molecule chelators and CAII variants. The metal ion affinities for the CAII variants were determined as described in the legend of Figure 2 and these values are listed in Table 1. The CAII variants included in this graph are wild-type (○), H94D (▼), H94Q (□), H119N (▲), and H119Q (◆). Some of the values of −log K_D are maximum values, as indicated by the ↓ symbol. Inset: Metal dissociation constants (K_D) for small molecule chelators, including bicine (✣), DPA (●), and 8-hydroxyquinoline-5-sulfonate (△), are taken from the National Institute of Standards and Technology Standard Reference Database 46.

reduces Zn^{2+} affinity much more than the affinity for any other ion. For example, the Cu^{2+} affinity of the majority of CAII variants, relative to WT CAII, is decreased 10^2−10^3-fold while the Zn^{2+} affinity is decreased 10^5−10^6-fold (Table 1). The smallest perturbations in metal ion affinities are observed for the H94D variant where Ni^{2+} binding is unaffected and the affinity for Co^{2+}, Cu^{2+}, and Cd^{2+} is diminished by ∼3-, 47-, and 2-fold, respectively. However, this substitution still reduces Zn^{2+} affinity substantially (>5000-fold). In this regard, H94D is typical of the variants, confirming the earlier assertion that CAII has selectivity for Zn^{2+}. WT CAII is Zn^{2+}-specific not only relative to the small molecule chelators but also relative to the CAII metal ligand variants.

Inherent Metal Ion−*Ligand Affinity Trend: The Irving*−*Williams Series*. The metal ion affinities of almost all of the variants examined follow the Irving−Williams series (Mn^{2+} < Co^{2+} < Ni^{2+} < Cu^{2+} > Zn^{2+}) (*2*), and are also in-line with the related MC series in that the Cd^{2+} affinity is close to that of Zn^{2+} and Ni^{2+} in the Irving−Williams series (*28*). The sole exception to this rule is H119Q CAII, which has equal to or higher affinity for Zn^{2+} than for Cu^{2+} (Table 1, Figure 3). In general, the ratios of affinities for the various metal ions of the CAII variants much more closely approximate the ratios measured for small molecule chelators than the ratios observed for WT CAII. These data indicate that wild-type CAII shows enhanced specificity for Zn^{2+} relative to Cu^{2+}, even though it does not violate the Irving−Williams series. This similarity in affinity ratios between small molecule chelators and the CAII variants can be seen by comparing the metal ion affinity profile of the H94D, H94Q, and H119N CAII variants (Figure 3) with that of small molecule chelators (Figure 3, inset). Additionally, the negative log of the K_D (i.e., the pK_D) of small molecule chelators (*18*) correlates well with the second ionization enthalpy (*3*) of the metal ions (e.g., the *R*-factor for the linear fit of the pK_D of nitrilotriacetic acid vs ΔH_{ion} is 0.96) (data not shown), indicating that this is a reasonable parameter by which to measure Irving−Williams-type behavior. Similarly, the metal pK_Ds for the CAII proteins examined, except for WT CAII and H119Q CAII, also correlate well with the second ionization enthalpy (e.g., the *R*-factors of H94Q and H119N CAII are both 0.93) (data not shown). The lower correlation observed between the metal ion affinity and the second ionization enthalpy for WT and H119Q CAII (*R*-factors of 0.86 and 0.7, respectively) reflects deviations from the Irving−Williams series, mainly caused by the enhanced Zn^{2+} affinity. These data suggest that the Irving−Williams series represents an inherent metal ion−ligand affinity trend which is equally applicable to small molecule chelators and metal binding sites in proteins, although deviations from this underlying trend can occur. Furthermore, this result suggests that a low correlation between the pK_D and the second ionization enthalpy for various metals can be used to identify proteins in which metal-ion-specific interactions occur.

Surprisingly, other than the second ionization enthalpy of the metal, there is no easily quantifiable parameter that correlates with the metal ion affinity of these variants. Linear correlations between the pK_D of the divalent metal ion and the side chain hydrophobicity, hydrophilicity, volume, surface area, pK_a, p*I*, or relative polarity of the substituted side chain (*29*) all yield a scatter plot with an *R*-factor <0.5 (data not shown).

Charge. Ligand charge has been suggested to play a role in metal affinity and specificity (*21*, *30*). To test this hypothesis, we compared the metal ion affinity of variants containing a metal polyhedron with a neutral metal ligand (Asn or Gln) to that of variants with a negatively charged ligand (Asp or Glu). Surprisingly, these data show no consistent trend, indicating that the charge on the ligand is *not* a major determinant in metal affinity in the CAII metal

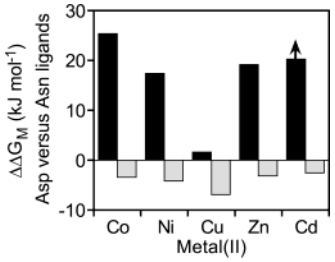

FIGURE 4: Dependence of the metal ion affinity on the charge of the coordinating ligand. Comparison of the metal affinity of CAII variants containing an uncharged metal ligand (Asn) compared to a charged ligand (Asn), where $\Delta\Delta G_M = RT \ln(K_{D,Asn}) - RT \ln(K_{D,Asp})$. The values of K_D are taken from Table 1. A positive $\Delta\Delta G_M$ indicates that the metal ion binds more tightly to the variant containing the charged side chain while a negative $\Delta\Delta G_M$ indicates enhanced affinity with the neutral side chain. The black bars represent comparisons of the affinity of mutations at position 94, and the gray bars indicate comparisons of variants at position 119. The arrow indicates that the value of $\Delta\Delta G_M$ is a lower limit. No consistent preference for charged or neutral ligands is observed for any of the metal ions.

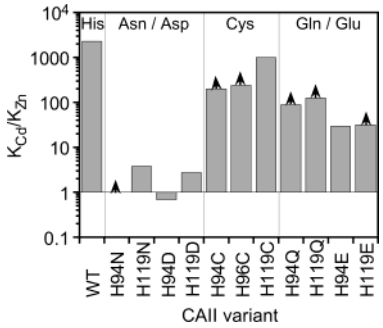

FIGURE 5: Metal ion selectivity (K_{Cd}/K_{Zn}) of CAII variants. The metal ion selectivity of CAII variants for Cd^{2+} relative to Zn^{2+} (K_{Cd}/K_{Zn}) is plotted. The values of K_{Cd} and K_{Zn} are taken from Table 1. A larger value for K_{Cd}/K_{Zn} indicates higher selectivity for Zn^{2+} while a smaller value indicates enhanced selectivity for Cd^{2+}. The variants are separated by both polarizability of the liganding atom and length of the side chain. The Asn and Gln variants coordinate metal with an uncharged carbonyl oxygen, the Asp and Glu variants coordinate metal with a carboxylate oxygen, and the Cys variants coordinate metal with the more polarizable thiolate atom.

polyhedron. At position 94, variants with the charged group Asp have higher affinity for all metals than variants containing the neutral ligand Asn (Table 1; Figure 4). In contrast, at position 119 the result is reversed; variants with the neutral Asn side chain have higher affinity for all metal ions than variants containing a negatively charged Asp. This was an unexpected result and suggests that the position of the side chain has a stronger effect on metal affinity than the charge on the coordinating group. The metal−ligand positioning at these two positions is different since zinc coordinates the ϵ and δ nitrogen of H94 and H119, respectively. Similarly, variations are observed for the relative metal affinity of variants containing a Glu versus a Gln ligand, although the high dependence on the position of the side chain is not conserved. For example, at position 119 the variant with the charged Glu side chain has much higher affinity for Cu^{2+} compared to H119Q CAII while the uncharged side chain in the H94Q variant confers higher affinity for Ni^{2+} compared to H94E CAII. These data demonstrate that there is no consistent, proportional preference for charged or neutral ligands in this metal binding site and, therefore, factors other than electrostatic interactions must be major determinants of the metal affinity.

Polarizability. One hypothesis for altering metal ion specificity is Pearson's hard−soft/acid−base rules which state that soft, or highly polarizable, metals tend to associate more strongly with soft ligands and hard, or not very polarizable, metals tend to associate more strongly with hard ligands (*31*). To investigate the role of side chain polarizability in determining the metal ion specificity in CAII, we compare the affinity of the borderline Zn^{2+} with that of the polarizable, soft Cd^{2+} for variants containing either a hard carbonyl oxygen (Asn or Gln), a slightly more polarizable carboxyl oxygen (Asp or Glu), or a soft sulfur-liganding atom (Cys). The substitution of Cys for a His ligand significantly decreases the affinity of CAII for both Zn^{2+} and Cd^{2+}, and in fact, the affinity for Cd^{2+} is too weak to be measured accurately in many cases (Table 1). Nonetheless, the metal ion selectivity ratio (K_{Cd}/K_{Zn}) remains large (≥200-fold) for the His_2Cys metal polyhedra, indicating that Zn^{2+} still binds with higher affinity than Cd^{2+} (Figure 5). The His to Cys substitution increases specificity for Cd^{2+}, relative to wild-type CAII, at most 10-fold [calculated from $(K_{Cd}/K_{Zn})^{WT}/(K_{Cd}/K_{Zn})^{Mu}$]. In contrast, substitution of His by Asn or Asp, amino acids that coordinate metals with an oxygen atom but retain the chain length of Cys, causes a larger decrease, on average, in the Zn^{2+} affinity than the Cd^{2+} affinity. Therefore, the metal ion selectivity ratio (K_{Cd}/K_{Zn}) decreases to less than 5, indicating that Zn^{2+} and Cd^{2+} bind with similar affinities in these variants (Table 1, Figure 5). Thus, the His to Asx substitution increases selectivity for Cd^{2+} relative to wild-type CAII [$(K_{Cd}/K_{Zn})^{WT}/(K_{Cd}/K_{Zn})^{Mu}$] by 600−3300-fold. In summary, the proteins with the harder oxygen ligands have higher selectivity for the softer metal ion (Cd^{2+}) than the variants with the softer sulfur ligands. (The metal selectivity comparisons for mutations containing a Glu or Gln compared to a Cys substitution are attenuated due to the additional change in the size of the metal polyhedron. These data are discussed further in the next section.) Since substitution of sulfur ligands for borderline ligands does not increase discrimination in favor of soft metal ions, Pearson's hard−soft/acid−base rules are not followed, and liganding atom polarizability is not the major determinant of metal ion specificity in the CAII binding site. The hard−soft/acid−base hypothesis is a poor indicator of metal ion specificity trends in CAII and, perhaps, more generally in proteins. In contrast, metal ion selectivity in a designed peptide scaffold can largely be explained by the donor atom preference for each metal ion (*32*). This difference is likely due to additional structural constraints imposed on the metal binding sites in proteins.

Site Size. Another hypothesis is that the size of the metal ion binding site can influence the metal selectivity (*10*); for example, a larger site may favor the binding of a large ion over that of a small ion. Here we examine the binding of metals with ionic radii ranging from 0.83 Å (6-coordinate Ni^{2+}) to 1.09 Å (6-coordinate Cd^{2+}) in a site where the native ion, Zn^{2+}, has an intermediate ionic radius (0.88 Å) (*3*). In this analysis we assume that, as a first approximation, longer side chains (Glx) produce a smaller binding site and shorter side chains (Asx being ~20 Å^3 smaller than Glx side chains, on average) produce a larger binding site. An examination of the crystal structures of these variants (*21*, *33*, *34*) indicates

Table 2: Geometries and Distances in the Zinc-Binding Polyhedra of Carbonic Anhydrase Variants

		distance of liganding atom from zinc ion (Å)				
variant	geometry	position 94	position 96	position 119	nonprotein 1	nonprotein 2
WT CAII[a]	tetrahedral	2.1	2.1	2.1	2.1 (Wat)[b]	NA
H94D[c]	distorted trigonal bipyramidal	2.1	2.4	2.2	2.4 (Wat)	2.6 (Wat)
H94E[d]	distorted tetrahedral	2.3	2.4	2.3	2.5 (Wat)	NA
H94N·Tris[e]	distorted trigonal bipyramidal	2.0	2.1	2.0	2.3 (Tris)	2.4 (Tris)
H94N·Azm[e,f]	distorted trigonal bipyramidal	2.0	2.0	2.0	2.1 (Azm)[e]	2.9 (Azm)[e]
H119D[g]	distorted trigonal bipyramidal	2.2	2.0	2.8	2.2 (Wat)	2.4 (Wat)
H119N[e]	trigonal bipyramidal	2.0	2.0	2.3	2.1 (Wat)	2.2 (Wat)
H119Q[e]	distorted tetrahedral	2.1	2.0	1.9	2.3 (Wat)	NA

[a] Reference *9*. [b] Wat is water or H_2O. [c] Reference *33*. [d] Reference *35*. [e] Reference *21*. [f] Azm is acetazolamide or *N*-(5-sulfamoyl-1,3,4-thiadiazol-2-yl)acetamide. [g] Reference *34*.

that this simple model is reasonable; the liganding atoms of the side chains are an average of 3.5−3.6 Å away from one another in H119D and H94D CAII, but only ~3.1 Å away from one another in H119Q CAII.

The only metal ion we examined that has a significantly larger ionic radius than Zn^{2+} is Cd^{2+} (*3*). As may be seen in Figure 5, the size of the substituted side chain does influence the binding selectivity for Cd^{2+} vs Zn^{2+}; sites with shorter side chains (compare D with E and N with Q) have higher selectivity for Cd^{2+} (lower K_{Cd}/K_{Zn}), although the effect is modest (~34-fold, on average). Examining the wild-type CAII crystal structure, we note that the Cα−Zn^{2+} distances at positions 94 (6.1 Å) and 119 (5.0 Å) are somewhat different, due to the liganding atom being the Nϵ2 nitrogen in H94 and the Nδ1 nitrogen in H119. Therefore, substitution of a shorter side chain at position 94 results in a slightly larger binding site than an equivalent substitution at position 119. This is reflected in the slightly lower K_{Cd}/K_{Zn} ratios (Table 1, Figure 5). These are modest effects, but, nonetheless, decreasing the length of a side chain and therefore increasing the size of the metal binding site causes a larger enhancement in Cd^{2+} selectivity than does altering the polarizability of the liganding atom. However, the selective influence of site size is only apparent where a comparison of isoelectronic ions is made. No clear size-related trend is present when nonisoelectric ions are compared (Table 1), suggesting that factors related to the electron shell occupancy may play a larger role in metal ion selectivity than size matching.

Site Geometry. None of the previously examined parameters appear to be a primary determinant of metal ion selectivity in CAII. To examine whether the geometry of the metal binding site in CAII is important for metal selectivity, we compare the thermodynamic metal ion affinity data with the metal site geometry visualized in protein crystal structures, as summarized in Table 2 (*9*, *21*, *33*−*35*). The crystal structure of H119N CAII demonstrates that the geometry of bound Zn^{2+} ion changes to trigonal bipyramidal (from tetrahedral in wild-type CAII) due to the binding of an additional solvent molecule to the Zn^{2+} ion (*21*). Since the geometry of Cu^{2+} is trigonal bipyramidal in wild-type CAII, changes in the protein structure that stabilize this geometry relative to other geometries are predicted to enhance Cu^{2+} affinity. This prediction is confirmed for the metal selectivity of H119N CAII (Figure 3, Table 1); the ratio of the metal dissociation constants (K_{Cu}/K_{Zn}) changes dramatically from a modest 8-fold preference for Cu^{2+} in wild-type CAII to ~31000-fold higher affinity for Cu^{2+} in H119N CAII. This preference pattern holds true for each of the other variants in which the crystal structure illustrates a trigonal bipyramidal Zn^{2+} binding site (Table 2), including H94N (1×10^6-fold) (*21*), H119D (7000-fold) (*34*), and H94D (1000-fold) (*33*). This correlation suggests that geometric constraints are important for modulating the Cu^{2+}/Zn^{2+} selectivity in CAII. Since the majority of variants demonstrate both enhanced Cu^{2+} selectivity and trigonal bipyramidal Zn^{2+} binding sites, it is likely that the protein structure in wild-type CAII stabilizes the tetrahedral geometry observed for Zn^{2+} while destabilizing the trigonal bipyramidal geometry. Nonetheless, the wild-type binding site does not enforce tetrahedral geometry, as illustrated by the diverse geometries observed in the crystal structures of metal-substituted CAII (*8*, *9*).

In contrast, the crystal structure of H119Q CAII (*21*) illustrates a highly constrained, slightly distorted tetrahedral Zn^{2+} binding. The glutamine side chain shifts the position of the bound Zn^{2+} by 0.74 Å compared to wild-type CAII. This movement decreases the available space for additional coordinating water molecules and alters the position of the Zn^{2+}-bound water so that it no longer is able to form a hydrogen bond with the side chain of T199. The enormous decrease in metal affinity (Table 1) is likely due to a combination of the loss of this hydrogen bond and the alteration of the position of the metal ion. On the basis of the trends in liganding number and geometry, the H119Q variant is predicted to have enhanced selectivity for Zn^{2+}, as Zn^{2+} prefers a relatively low coordination number (4) and tetrahedral geometry. A comparison of the metal ion specificity of H119Q CAII with its short side chain analogue, H119N CAII, is particularly striking; the affinity of H119Q CAII for Zn^{2+} is decreased modestly (6-fold) while the Cu^{2+} affinity is diminished >200000-fold, leading to a significant enhancement in Zn^{2+} selectivity. Similarly, H119Q CAII has enhanced selectivity for Zn^{2+} (K_M/K_{Zn}) relative to the H119N CAII for Co^{2+} (>20-fold), Ni^{2+} (>26-fold), and Cd^{2+} (>32-fold). Importantly, the effect of the geometric constraint is apparently strong enough to cause H119Q CAII to violate the Irving−Williams series (Figure 3), by having higher affinity for Zn^{2+} than for Cu^{2+}. These data indicate that the metal ion affinity alterations in H119Q CAII can be largely explained by alterations in the geometric constraints on the metal ion polyhedron.

Previous mutagenesis studies also suggest that copper/zinc selectivity in CAII is related to the geometry of the metal binding site (*36*, *37*). Amino acid substitutions in hydrophobic residues located underneath the metal ion binding site

of CAII (Figure 1, F_{93}, F_{95}, and W_{97}) enhance Cu^{2+} affinity while decreasing Co^{2+} and Zn^{2+} affinity (*38*). X-ray crystal structures of metal-bound CAII variants reveal that the tetrahedral Zn^{2+} and trigonal bipyramidal Cu^{2+} coordination geometry is retained (*37*). However, in the apoenzyme a conformational change of the direct metal ligand H94 as well as the indirect (i.e., "second-shell") ligand Q92 is observed, thereby eliminating preorientation of the histidine ligands with tetrahedral geometry in the apoenzyme. Therefore, these aromatic core residues serve as anchors that help to preorient direct and second-shell ligands to optimize the tetrahedral Zn^{2+} binding geometry and to destabilize alternative geometries. These data, along with the current studies, suggest that geometrical constraints are a main determinant of the enhanced zinc/copper selectivity of CAII compared to small molecule chelators.

Importance of Stabilizing Hydrogen Bonds. In contrast, the metal ion specificity and affinity of the H94D CAII site are difficult to rationalize solely on the basis of geometric alterations observed in the crystal structures. Although the H94D site is trigonal bipyramidal with Zn^{2+} bound, the metal selectivity profile does not parallel that of H119N (Figure 3) or H119D CAII (Table 1). In fact, H94D has the highest overall affinity of all of the CAII variants (with an affinity for Co^{2+}, Ni^{2+}, and Cd^{2+} comparable to that of wild-type CAII) and is the only variant with higher affinity for Cd^{2+} than for Zn^{2+} (by ~1.5-fold). The H94D crystal structure visualizes the formation of an additional hydrogen bond between one of the metal-liganding solvent molecules (*33*) and the non-metal-ligand oxygen of Asp that is presumably responsible for the unusually high metal affinity of this variant. Stabilizing hydrogen bonds may also explain the enhanced metal affinity of other variants as well. For example, the crystal structures indicate that H119N, but not H119D, CAII retains the second shell hydrogen bond between the side chain of Glu117 and the amino acid side chain at position 119. This hydrogen bond likely explains the ~10-fold higher metal ion affinity of H119N CAII compared to that of H119D, consistent with the enhancement of metal affinity by second shell hydrogen bonds in the His_3 CAII metal polyhedron (*39*). Therefore, introducing stabilizing hydrogen bonds may be a generic method for improving metal ion affinity and selectivity in designed proteins (*40*, *41*). High selectivity for Zn^{2+} was recently observed in a designed tetrahedral zinc binding site that included second shell hydrogen bonds (*41*).

Activity. Studies of the catalytic activity of the metal-substituted wild-type CAII demonstrate that only the metals able to easily adopt a tetrahedral coordination sphere, Zn^{2+} and Co^{2+}, provide significant catalytic enhancement (*8*). For CAII mutants containing substitutions in the His ligands, the Zn^{2+}-bound enzymes all catalyze *p*-nitrophenyl acetate hydrolysis to varying degrees, as indicated by the pH-independent k_{cat}/K_M; however, the catalytic pK_a is markedly higher in the carboxyl-substituted variants (*20*, *21*). In the case of the carboxamide-substituted variants, the pK_a of the reaction is not as highly perturbed, but the k_{cat}/K_M values for either PNPA hydrolysis or CO_2 hydration are still depressed relative to wild type (*21*). The only carboxamide-substituted variant retaining a tetrahedral Zn^{2+} coordination sphere, H119Q CAII, is also the variant with the least perturbed pK_a (6.9, as compared to 6.8 for wild-type CAII). This correlation is consistent with the prediction that lower coordination numbers are important for both depressing the pK_a and increasing the reactivity of Zn^{2+}-bound solvent (*42*). Therefore, while the histidine ligands are not essential for catalytic activity, they are likely conserved not only for metal ion selectivity but also to maximize electrostatic stabilization of both the ground-state zinc hydroxide and the negatively charged transition state at physiological pH (*20*).

CONCLUSIONS

This work has been the first examination of the metal ion specificity of a library of closely related metal ion polyhedra. By determining the metal ion binding affinity of a number of CAII variants for a range of metal ions, we were able to directly test four hypotheses of metal ion specificity: inherent ligand affinity, polarizability, site size, and geometry. Wild-type CAII and almost all of the variants follow the inherent metal ion affinity trend suggested by the Irving−Williams series, demonstrating that the inherent metal ion affinity trend operates within proteins as well as within small molecule chelators and may be a dominant factor in metal ion affinity in biology. This tendency of the variants to follow an inherent metal ion−ligand affinity series strongly implies that, for biology to impose specificity, it must compete with the inherent ligand affinity trends described by the Irving−Williams series. H119Q CAII did not follow the Irving−Williams series, demonstrating that it is possible for other influences within a protein to overcome this trend. Neither the polarizability of the liganding side chains nor the size of the metal ion binding site strongly affects metal ion specificity in our study, although the size of the site may aid in discrimination between isoelectric ions. Instead, changes in metal ion specificity of the variants can be tied directly to the preferred coordination number and geometry of the metal ion. Therefore, modulation of the ability of a bound metal ion to adopt its preferred coordination number/geometry appears to be the primary feature driving deviations from the inherent ligand affinity trend in CAII and likely other proteins as well.

ACKNOWLEDGMENT

We thank Dr. David W. Christianson and Charles Lesburg for solving and providing insight into the structures of many of the CA variants.

REFERENCES

1. Lippard, S. J., and Berg, J. M. (1994) *Principles of Bioinorganic Chemistry*, pp 1−20, University Science Books, Mill Valley, CA.
2. Irving, H., and Williams, R. J. P. (1948) Order of Stability of Metal Complexes, *Nature 162*, 746−747.
3. Cotton, F. A., and Wilkinson, G. (1988) *Advanced Inorganic Chemistry: a Comprehensive Text*, 5th ed., pp 1381−1382 and 1385−1388, John Wiley & Sons, New York.
4. Pearson, R. G. (1966) Acids and Bases, *Science 151*, 172−177.
5. Pearson, R. G. (1968) Hard and Soft Acids and Bases, HSAB, Part I, Fundamental Principles, *J. Chem. Educ. 45*, 581−587.
6. Cavet, J. S., Meng, W., Pennella, M. A., Appelhoff, R. J., Giedroc, D. P., and Robinson, N. J. (2002) A nickel-cobalt-sensing ArsR-SmtB family repressor. Contributions of cytosol and effector binding sites to metal selectivity, *J. Biol. Chem. 277*, 38441−38448.
7. Pennella, M. A., Shokes, J. E., Cosper, N. J., Scott, R. A., and Giedroc, D. P. (2003) Structural elements of metal selectivity in metal sensor proteins, *Proc. Natl. Acad. Sci. U.S.A. 100*, 3713−3718.

8. Hakansson, K., Wehnert, A., and Liljas, A. (1994) X-ray Analysis of Metal-substituted Human Carbonic Anhydrase II Derivatives, *Acta Crystallogr. D50*, 93−100.
9. Hakansson, K., and Wehnert, A. (1992) Structure of Cobalt Carbonic Anhydrase Complexed with Bicarbonate, *J. Mol. Biol. 228*, 1212−1218.
10. Glusker, J. P. (1991) Structural aspects of metal liganding to functional groups in proteins, *Adv. Protein Chem. 42*, 1−76.
11. Rulisek, L., and Vondrasek, J. (1998) Coordination geometries of selected transition metal ions (Co^{2+}, Ni^{2+}, Cu^{2+}, Zn^{2+}, Cd^{2+}, and Hg^{2+}) in metalloproteins, *J. Inorg. Biochem. 71*, 115−127.
12. Hellinga, H. W., and Richards, F. M. (1991) Construction of New Ligand Binding Sites in Proteins of Known Structure: I. Computer-aided modeling of sites with pre-defined geometry, *J. Mol. Biol. 222*, 763−785.
13. Rypniewski, W. R., Mangani, S., Bruni, B., Orioli, P. L., Casati, M., and Wilson, K. S. (1995) Crystal structure of reduced bovine erythrocyte superoxide dismutase at 1.9 Å resolution, *J. Mol. Biol. 251*, 282−296.
14. Tainer, J. A., Getzoff, E. D., Beem, K. M., Richardson, J. S., and Richardson, D. C. (1982) Determination and analysis of the 2 Å structure of copper, zinc superoxide dismutase, *J. Mol. Biol. 160*, 181−217.
15. McCall, K. A., and Fierke, C. A. (2000) Colorimetric and fluorimetric assays to quantitate micromolar concentrations of transition metals, *Anal. Biochem. 284*, 307−315.
16. Lindskog, S., and Nyman, P. O. (1964) Metal-binding Properties of Human Erythrocyte Carbonic Anhydrases, *Biochim. Biophys. Acta 85*, 462−474.
17. Kidani, Y., and Hirose, J. (1977) Coordination Chemical Studies on Metalloenzymes: II. Kinetic Behavior of Various Types of Chelating Agents Towards Bovine Carbonic Anhydrase, *J. Biochem. 81*, 1383−1391.
18. Motekaitis, R. J. (1977) U.S. Department of Commerce, Technology Administration, National Institute of Standards and Technology, Standard Reference Data Program, College Station, TX.
19. Martensson, L.-G., Jonsson, B.-H., Freskgard, P.-O., Kihlgren, A., Svensson, M., and Carlsson, U. (1993) Characterization of Folding Intermediates of Human Carbonic Anhydrase II: Probing Substructure by Chemical Labeling of SH Groups Introduced by Site-Directed Mutagenesis, *Biochemistry 32*, 224−231.
20. Kiefer, L. L., and Fierke, C. A. (1994) Functional Characterization of Human Carbonic Anhydrase II Variants With Altered Zinc Binding Sites, *Biochemistry 33*, 15233−15240.
21. Lesburg, C. A., Huang, C.-c., Christianson, D. W., and Fierke, C. A. (1997) Histidine → Carboxamide Ligand Substitutions in the Zinc Binding Site of Carbonic Anhydrase II Alter Metal Coordination Geometry but Retain Catalytic Activity, *Biochemistry 36*, 15780−15791.
22. Alexander, R. S., Kiefer, L. L., Fierke, C. A., and Christianson, D. W. (1993) Engineering the Zinc Binding Site of Human Carbonic Anhydrase II: Structure of the His-94→Cys Apoenzyme in a New Crystalline Form, *Biochemistry 32*, 1510−1518.
23. Tu, C. K., and Silverman, D. N. (1982) Solvent Deuterium Isotope Effects in the Catalysis of Oxygen-18 Exchange by Human Carbonic Anhydrase II, *Biochemistry 21*, 6353−6360.
24. Coleman, J. E., and Vallee, B. L. (1961) Metallocarboxypeptidases: Stability Constants and Enzymatic Characteristics, *J. Biol. Chem. 236*, 2244−2249.
25. Piras, R., and Vallee, B. L. (1967) Procarboxypeptidase A-Carboxypeptidase A Interrelationships. Metal and Substrate Binding, *Biochemistry 6*, 348−357.
26. Tse, P., Scopes, R. K., and Wedd, A. G. (1989) Iron-Activated Alcohol Dehydrogenase from *Zymomonas mobilis*: Isolation of Apoenzyme and Metal Dissociation Constants, *J. Am. Chem. Soc. 111*, 8703−8706.
27. Van Dam, M. E., Wuenschell, G. E., and Arnold, F. H. (1989) Metal Affinity Precipitation of Proteins, *Biotech. Appl. Biochem. 11*, 492−502.
28. Martin, B. L. (1999) Development of a scale for the comparison of metals in enzyme action, *J. Inorg. Biochem. 75*, 245−254.
29. Creighton, T. E. (1983) *Proteins: structures and molecular principles*, pp 7 and 142, W. H. Freeman, New York.
30. Snyder, E. E., Buoscio, B. W., and Falke, J. J. (1990) Calcium-(II) site specificity: Effect of size and charge on metal ion binding to an EF-hand-like site, *Biochemistry 29*, 3937−3943.
31. Pearson, R. G. (1963) Hard and Soft Acids and Bases, *J. Am. Chem. Soc. 85*, 3533−3539.
32. Shults, M. D., Pearce, D. A., and Imperiali, B. (2003) Modular and Tunable Chemosensor Scaffold for Divalent Zinc, *J. Am. Chem. Soc. 125*, 10591−10597.
33. Kiefer, L. L., Ippolito, J. F., Fierke, C. A., and Christianson, D. W. (1993) Redesigning the Zinc Binding Site of Human Carbonic Anhydrase II: Structure of a His_2Asp-Zn^{2+} Metal Coordination Polyhedron, *J. Am. Chem. Soc. 115*, 12581−12582.
34. Ippolito, J. A., and Christianson, D. W. (1994) Structural Consequences of Redesigning a Protein-Zinc Binding Site, *Biochemistry 33*, 15241−15249.
35. Xue, Y., Jonsson, B.-H., Liljas, A., and Lindskog, S. (1994) Modification of a metal ligand in carbonic anhydrase: crystal structure of His94→Glu human isozyme II, *FEBS Lett. 352*, 137−140.
36. Hunt, J. A., and Fierke, C. A. (1997) Selection of Carbonic Anhydrase Variants Displayed on Phage: Aromatic Residues in Zinc Binding Site Enhance Metal Affinity and Equilibration Kinetics, *J. Biol. Chem. 272*, 20364−20372.
37. Cox, J. D., Hunt, J. A., Compher, K. M., Fierke, C. A., and Christianson, D. W. (2000) Structural influence of hydrophobic core residues on metal binding and specificity in carbonic anhydrase II, *Biochemistry 39*, 13687−13694.
38. Hunt, J. A., Ahmed, M., and Fierke, C. A. (1999) Metal Binding Specificity in Carbonic Anhydrase is Influenced by Conserved Hydrophobic Core Residues, *Biochemistry 38*, 9054−9062.
39. Kiefer, L. L., Paterno, S. A., and Fierke, C. A. (1995) Hydrogen Bond Network in the Metal Binding Site of Carbonic Anhydrase Enhances Zinc Affinity and Catalytic Efficiency, *J. Am. Chem. Soc. 117*, 6831−6837.
40. Marino, S. F., and Regan, L. (1999) Secondary ligands enhance affinity at a designed metal-binding site, *Chem. Biol. 6*, 649−655.
41. Dwyer, M. A., Looger, L. L., and Hellinga, H. W. (2003) Computational design of a Zn^{2+} receptor that controls bacterial gene expression, *Proc. Natl. Acad. Sci. U.S.A. 100*, 11255−11260.
42. Bertini, I., Luchinat, C., Rosi, M., Sgamellotti, A., and Tarantelli, F. (1990) pK_a of Zinc-Bound Water and Nucleophilicity of Hydroxo-Containing Species. *Ab Initio* Calculations on Models for Zinc Enzymes, *Inorg. Chem. 29*, 1460−1463.
43. Kraulis, P. J. (1991) MOLSCRIPT: A Program to Produce Both Detailed and Schematic Plots of Protein Structures, *J. Appl. Crystallogr. 24*, 946−950.
44. Merritt, E. A., and Bacon, D. J. (1997) Raster3D: Photorealistic Molecular Graphics, *Methods Enzymol. 277*, 505−524.

BI0498914